Molecular Cell
Article

Telomere Protection by TPP1/POT1 Requires Tethering to TIN2

Kaori K. Takai,[1] Tatsuya Kibe,[1,2] Jill R. Donigian,[1,2] David Frescas,[1] and Titia de Lange[1,*]
[1]Laboratory for Cell Biology and Genetics; The Rockefeller University; 1230 York Avenue; New York; NY 10065, USA
[2]These authors contributed equally to this work
*Correspondence: delange@mail.rockefeller.edu
DOI 10.1016/j.molcel.2011.08.043

SUMMARY

To prevent ATR activation, telomeres deploy the single-stranded DNA binding activity of TPP1/POT1a. POT1a blocks the binding of RPA to telomeres, suggesting that ATR is repressed through RPA exclusion. However, comparison of the DNA binding affinities and abundance of TPP1/POT1a and RPA indicates that TPP1/POT1a by itself is unlikely to exclude RPA. We therefore analyzed the central shelterin protein TIN2, which links TPP1/POT1a (and POT1b) to TRF1 and TRF2 on the double-stranded telomeric DNA. Upon TIN2 deletion, telomeres lost TPP1/POT1a, accumulated RPA, elicited an ATR signal, and showed all other phenotypes of POT1a/b deletion. TIN2 also affected the TRF2-dependent repression of ATM kinase signaling but not to TRF2-mediated inhibition of telomere fusions. Thus, while TIN2 has a minor contribution to the repression of ATM by TRF2, its major role is to stabilize TPP1/POT1a on the ss telomeric DNA, thereby allowing effective exclusion of RPA and repression of ATR signaling.

INTRODUCTION

Mammalian telomeres are comprised of numerous copies of shelterin, which are assembled on the telomeric TTAGGG repeat DNA (Palm and de Lange, 2008). Shelterin recognizes telomeres primarily with two duplex telomeric DNA-binding factors (telomeric repeat-binding factor 1 [TRF1] and TRF2). It also contains one (in humans) or two (in rodents) protection of telomeres protein 1 (POT1) proteins that bind to single-stranded (ss) TTAGGG repeats. The POT1 proteins connect to TRF1 and TRF2 through protein interactions involving TPP1 and TRF1-interacting protein 2 (TIN2) (Liu et al., 2004b; Houghtaling et al., 2004; Ye et al., 2004b), forming a multisubunit complex that can be isolated intact from human cells (Ye et al., 2004a; O'Connor et al., 2006).

TIN2 is a central component of shelterin that not only connects TPP1/POT1 to the other shelterin components but also stabilizes TRF1 and TRF2 on the duplex telomeric repeat array (Liu et al., 2004a; Ye et al., 2004a; Kim et al., 2004). TIN2 contributes to telomere length regulation but its precise role in telomere protection has not been established (Abreu et al., 2010; Ye and de Lange, 2004; Kim et al., 1999). The function of TIN2 is of particular interest because it is mutated in a subset of Dyskeratosis congenita patients (Savage et al., 2008; Walne et al., 2008; Tsangaris et al., 2008).

The role of TIN2 in connecting TPP1/POT1 to TRF1/2 is relevant to the regulation of telomerase-mediated telomere maintenance (Loayza and de Lange, 2003; Kim et al., 1999; Abreu et al., 2010). However, the significance of this link to telomere protection has not been established. Several authors have suggested that the TPP1/POT1 heterodimer protects telomeres in a manner that does not require its association with TIN2/TRF1/TRF2 (e.g., [Giraud-Panis et al., 2010; Baumann and Price, 2010; Flynn et al., 2011]). Here, we present evidence indicating that TIN2 is critical for the protective functions of TPP1/POT1.

The essential function of TPP1/POT1 is to prevent the ataxia telangiectasia mutated (ATM) and ataxia telangiectasia mutated and Rad3-related protein (ATR)-kinase-dependent DNA damage response. The risk of inappropriate activation of the ATR kinase is inherent to the structure of mammalian telomeres, which contain single-stranded TTAGGG repeats owing to the greater length of the 3′-ended strand of the telomeric repeat array. This 3′ overhang can be either single-stranded or loop back and invade the duplex telomeric TTAGGG repeats. In the latter configuration, called the t-loop, single-stranded TTAGGG repeats are exposed in a displacement loop (D-loop) at the base of the t-loop (McElligott and Wellinger, 1997; Makarov et al., 1997; Chai et al., 2006; Griffith et al., 1999). The length of the single-stranded telomeric DNA is estimated to be 40–400 nt (Chai et al., 2006; Zhao et al., 2008), which is sufficient for the binding of replication protein A (RPA), the sensor in the ATR pathway ([Zou and Elledge, 2003]; reviewed in Cimprich and Cortez [2008]).

RPA recruits ATR to short-stranded DNA (ssDNA) through an interaction with ATR-interacting protein (ATRIP) (Ball et al., 2005, 2007; Zou and Elledge, 2003; Kumagai et al., 2004; Namiki and Zou, 2006; Xu et al., 2008). Its three subunits (RPA70, RPA32, and RPA14) form a complex that binds ssDNA with a dissociation constant (Kd) of 10^{-9}-10^{-11} M (Wold, 1997). The optimal RPA binding site is 30 nt, whereas RPA forms an unstable complex on substrates of 8–10 nt (Lavrik et al., 1999; Kim et al., 1992; Sibenaller et al., 1998; Blackwell and Borowiec, 1994; Blackwell et al., 1996). In vitro, two RPA units bound to ~75 nt of DNA are sufficient to recruit ATRIP (Zou and Elledge,

2003), and in a *Xenopus* egg extract system, a 35 nt ssDNA gap can activate the ATR kinase, presumably by binding a single RPA (MacDougall et al., 2007). Based on this data, the telomeric 3′ overhang is of sufficient length to meet the minimal requirements for RPA-mediated ATR activation. Therefore, it was proposed that telomeres might repress ATR signaling by excluding RPA from their single-stranded moiety.

The ssDNA binding factor in shelterin, the TPP1/POT1 heterodimer, is the most likely candidate repressor of RPA. POT1 binds to 5′-(T)TAGGGTTAG-3′ with subnanomolar affinity (Lei et al., 2004; Loayza et al., 2004; Nandakumar et al., 2010). POT1 recognizes this site at the 3′ end, a double-stranded (ds)-ss junction, and internally, predicting that POT1 can bind along the 3′ overhang and also to the ssDNA in the D-loop (Loayza et al., 2004; Wang et al., 2007; He et al., 2006; Lei et al., 2004; Palm et al., 2009). The two mouse POT1 proteins (POT1a and POT1b) and human POT1 have similar sequence specificity and DNA affinity (He et al., 2006; Palm et al., 2009). DNA binding by human POT1 is enhanced by the N-terminus of TPP1, although TPP1 has no discernable DNA-binding activity by itself (Wang et al., 2007; Xin et al., 2007). The recruitment of POT1 to telomeres critically depends on its interaction with TPP1. Deletion of TPP1 or interference with the TPP1-POT1 interaction leads to a lack of POT1-binding to telomeres (Liu et al., 2004b; Ye et al., 2004b; Hockemeyer et al., 2007; Kibe et al., 2010). Thus, POT1 is likely to bind to ss telomeric DNA and function there as a TPP1/POT1 heterodimer.

Consistent with the RPA exclusion model, removal of POT1a/b from mouse telomeres results in rapid accumulation of RPA, induction of telomere dysfunction-induced foci (TIFs), and phosphorylation of Chk1 (Hockemeyer et al., 2006; Denchi and de Lange, 2007; Gong and de Lange, 2010). This DNA damage response, which occurs in G1 and S/G2, is dependent on the ATR kinase and TopBP1. Additional phenotypes of POT1a/b DKO cells include deregulation of the 3′ overhang length (a phenotype specific to POT1b deletion), polyploidization due to endoreduplication, metaphases with diplochromosomes, and a low frequency of sister telomere fusion (Wu et al., 2006; Hockemeyer et al., 2006, 2008; Davoli et al., 2010). When TPP1 is compromised, the same phenotypes arise, confirming that TPP1 is required for POT1 function (Hockemeyer et al., 2007; Kibe et al., 2010).

We envisaged at least three, but not mutually exclusive, ways in which TPP1/POT1 could exclude RPA from telomeres. First, TPP1/POT1 could be more abundant than RPA. Second, TPP1/POT1 could have a higher affinity for telomeric DNA than RPA, as was suggested recently (Arnoult et al., 2009). Third, TPP1/POT1 might be locally enriched and stabilized at telomeres through TIN2-mediated tethering to the other shelterin components. Here, we show that POT1 is significantly less abundant than RPA and does not have a greater affinity for telomeric DNA, even when bound to TPP1. Through conditional deletion of TIN2, we provide direct evidence that TPP1/POT1 require a connection to the TIN2/TRF1/TRF2 complex to repress ATR signaling. A second function of TIN2 is to promote the repression of ATM signaling, but not nonhomologous end-joining, by TRF2.

RESULTS

RPA Is Significantly More Abundant Than the POT1 Proteins

The abundance of RPA and POT1a/b were determined through quantitative immunoblotting of whole cell lysates using known quantities of purified trimeric RPA and mouse POT1a and POT1b as standards (Figure S1 available online) (Takai et al., 2010). The result indicated that the HeLa1.3 and HTC75 tumor cell lines contained 3–5 million RPA molecules per cell (Figure 1A). This estimate is an order of magnitude higher than the previous estimates from DNA-binding and DNA replication assays using cytosolic and freeze/thaw lysates (Wold and Kelly, 1988; Seroussi and Lavi, 1993; Kenny et al., 1990). In contrast, POT1a and POT1b were each expressed at only 2–7 thousand molecules per mouse embryo fibroblast (MEF) cell (Figure 1B and Figure S1). This is consistent with the estimate of $\sim 2 \times 10^4$ copies of the single human POT1 in HeLa and HTC75 (Takai et al., 2010). Assuming that RPA is expressed at the same level in mouse and human cells, these data suggest that the mouse and human POT1 proteins are considerably less abundant than RPA.

RPA and TPP1/POT1 Have Similar Affinities for Telomeric DNA

To determine whether POT1 has a higher affinity for telomeric DNA than RPA, we first used baculovirus-derived human POT1 and human RPA purified from *E. coli*. The substrate was a telomeric repeat array of 34 nt (Tel34), which is sufficiently long to accommodate RPA and contains five overlapping POT1 recognition sites, including the optimal POT1 binding site at the 3′ end (TTAGGGTTAG-3′). Formation of G4 structures in the Tel34 probe were prevented by boiling immediately before use and inclusion of LiCl rather than NaCl or KCl in the reaction buffer. RPA showed the same subnanomolar affinity for Tel34, a scrambled 34 nt probe, and dT34 (Figures 1C–E). Tel34 was bound by two POT1 units in a noncooperative manner, whereas no POT1 binding was observed with the nontelomeric DNAs (Figures 1C and 1E). Importantly, the affinity of RPA and POT1 for the Tel34 was similar, on the order of 0.5–0.7 nM (Figure 1E), which concurs with previous data on RPA (Kim et al., 1992, 1994; Miyake et al., 2009).

To compare RPA to TPP1/POT1, we used mouse TPP1/POT1a (Figure S1) and human RPA. This cross-species comparison is justified because human and mouse RPA are virtually identical. Human and mouse RPA70, which contain four of the five oligonucleotide/oligosaccharide-binding (OB)-folds that mediate DNA-binding of RPA, are identical. Within RPA32, which contributes the fifth OB-fold involved in DNA binding, only 11% of the amino acids are different.

Mouse TPP1/POT1a was purified and the presence of the TPP1/POT1a complex was confirmed by immunoblotting and gel filtration (Figures S1C and S1D). Although the stoichiometry of POT1a and TPP1 could not be discerned from Coomassie-stained gels due to the diffuse pattern of TPP1 (Figure S1B), antibody super-shift experiments established the presence of TPP1 in the two complexes that formed on Tel34 (Figures 1D and S1E). These complexes likely contain POT1a as well because TPP1 does not bind DNA on its own. As expected, TPP1/POT1a

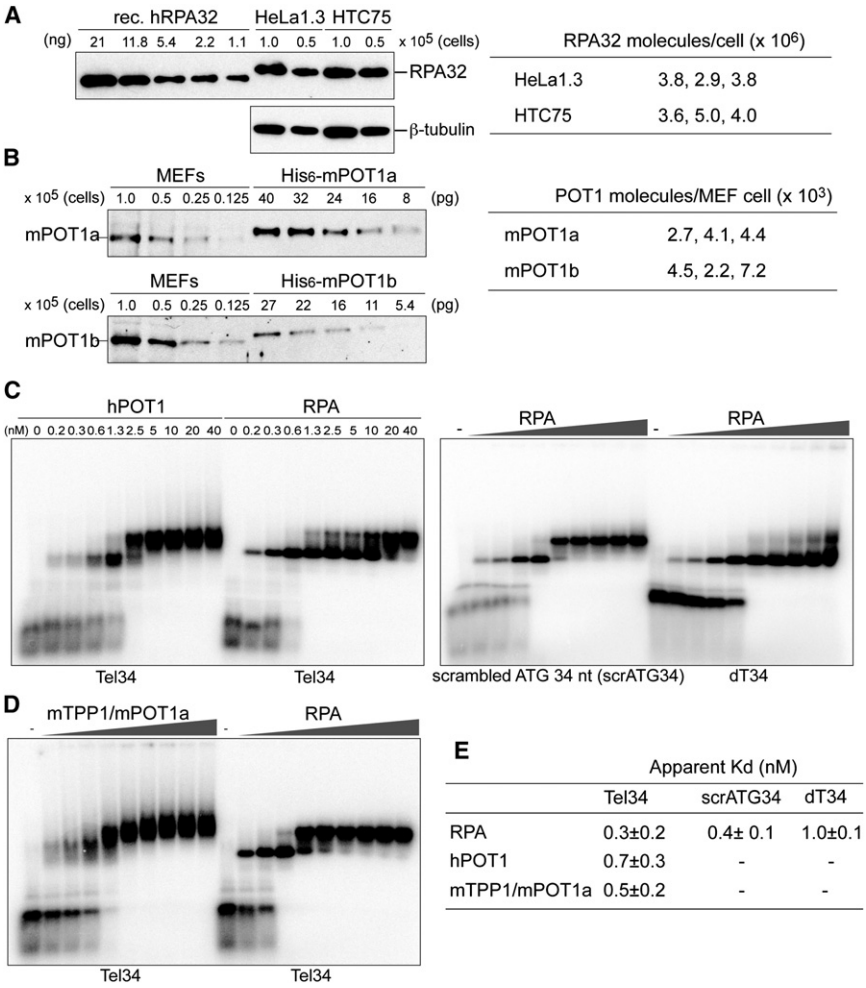

Figure 1. Abundance and DNA-Binding Features of POT1, TPP1/POT1a, and RPA

(A) and (B) Quantitative immunoblotting for RPA32, POT1a, and POT1b in whole cell lysates and comparison to recombinant standards (Figure S1A). Right: abundance of human RPA and mouse POT1a/b based on data from three experiments as shown on the left.

(C) Gel shift reactions with the indicated probes and increasing amounts (0.16-40 nM) of human POT1 or RPA.

(D) Binding of mouse TPP1/POT1a and human RPA to Tel34. Protein amounts as in (C).

(E) Summary of the apparent K_d of human RPA, human POT1, and mouse TPP1/POT1a derived from gel shift experiments as shown in (C) and (D) (average values from three experiments represented and standard deviations). K_d values were derived from mathematical curve fitting (GraphPad Prism) of PhosphorImager data on RPA and POT1 analyzed in parallel.

showed a higher affinity for telomeric DNA than POT1a alone and retained a preference for a 3′ end (Figures S1F and S1G).

Despite the improved DNA-binding affinity of TPP1/POT1a, side-by-side comparison revealed that RPA and TPP1/POT1a bound Tel34 with similarly apparent affinity (~0.5 nM) (Figures 1D and 1E). Together with the much greater abundance of RPA, these data suggest that the intrinsic properties of TPP1/POT1 are unlikely to prevent the binding of RPA to telomeric DNA in vivo.

TIN2 Loads TPP1/POT1 onto Telomeres

Given these biochemical data, we explored the possibility that TPP1/POT1 might require their interaction with TIN2 to compete with RPA. This hypothesis predicts that deletion of TIN2 elicits the phenotypes associated with loss of POT1a/b. As deletion of TIN2 results in embryonic lethality (Chiang et al., 2004), we generated conditional TIN2-knockout MEFs to determine the outcome of TIN2 loss (Figure 2). The TIN2 locus was modified by gene targeting, resulting in the insertion of loxP sites before exon 3 and after exon 7 (Figure 2A). The deletion of exons 3–7 generates a gene that encodes only the first 93 amino acids (aa) of TIN2 from exons 1 and 2. mRNA splicing from exon 2 to exon 8 creates a frameshift at the splice junction and premature termination of the ORF 12 amino acid into exon 8. Therefore, the TIN2$^{\Delta ex3-7}$ allele is expected to encode a severely truncated TIN2 lacking most of the protein, including the TRF1 binding site in exon 6 (Figure 2A).

Fibroblasts from E13.5 TIN2$^{F/F}$ embryos were immortalized with SV40 large T antigen and tested for the expected Cre-mediated recombination by genomic PCR (Figure 2A). Deletion of TIN2 induced a senescence-like growth arrest that was negated by exogenous mouse TIN2, indicating that the phenotype resulted from TIN2 loss (Figures S2A–S2D). Indirect immunofluorescence (IF) demonstrated the anticipated loss of telomeric TIN2 signals from these cells (Figure 2B), and the telomeric chromatin immunoprecipitation (ChIP) suggested that TIN2 levels at telomeres were reduced by ~20-fold (Figure 2C).

TIN2 was previously shown to promote the association of human TRF1 and TRF2 with telomeres (Ye et al., 2004a; Kim et al., 2004; O'Connor et al., 2006). In agreement, the TRF2 and Rap1 telomeric ChIP values diminished ~3-fold, whereas the TRF1 value was 4-fold lower (Figure 2C). The IF signals for TRF1 and TRF2 at telomeres were also diminished, and although TRF1, TRF2, and Rap1 continued to be chromatin-bound, the overall level of TRF1 detectable in immunoblots was lowered (Figures 2D and 2E).

To establish the effect of TIN2 on the telomeric localization of TPP1 and POT1a, oncogene (Myc)-tagged versions were introduced into TIN2$^{F/F}$ MEFs, where they showed the anticipated telomeric localization (Figures 2F and 2I). Both Myc-TPP1 and Myc-POT1a lost their telomeric localization after deletion of TIN2, despite unaltered expression (Figures 2F and 2I). Furthermore, based on ChIP, the telomeric association of TPP1 and

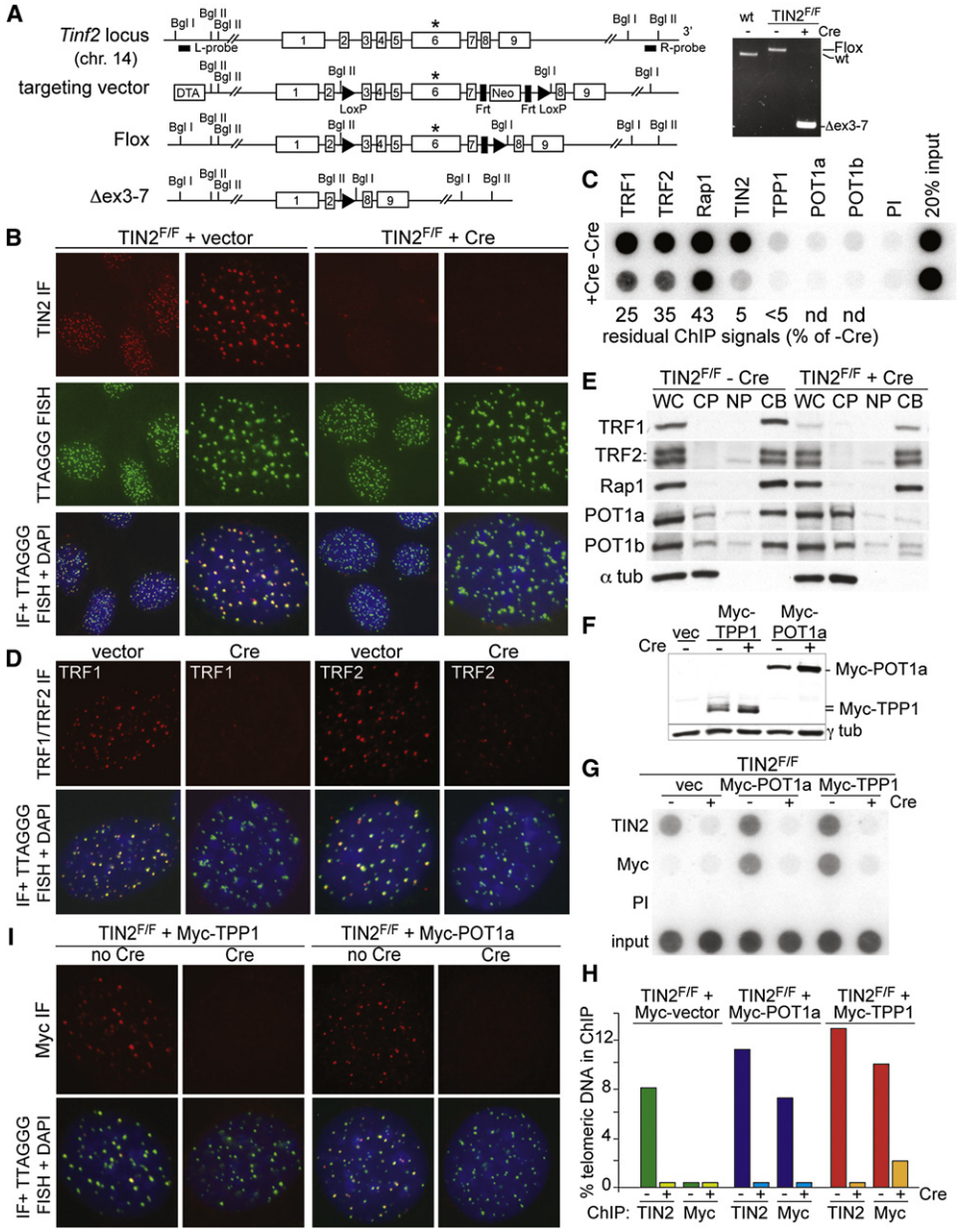

Figure 2. Conditional Deletion of TIN2

(A) Schematic showing the *Tinf2* genomic locus, the targeting construct, and the alleles generated. Black triangles, LoxP sites with *Bgl*I/BglII sites; black boxes, Frt sites; Neo, PGK-Neo gene; DTA, MCI-DTA; black bars, probes for genomic blotting; asterisk, TRF1 interaction motif in exon 6. Right: PCR genotyping of $TIN2^{+/+}$ and $TIN2^{F/F}$ MEFs after introduction of Cre.

(B) Loss of telomeric TIN2 signals from $TIN2^{F/F}$ MEFs treated with pWZL-Cre (92 h). IF for TIN2 (Ab 1447, red) at telomeres detected by FISH (green).

(C) Telomeric DNA ChIP for shelterin proteins in $TIN2^{F/F}$ MEFs with or without Cre treatment (92 h). ChIP signals were normalized to the input and the background (PI) was subtracted. Numbers below represent the average decrease in these values after deletion of TIN2 (two experiments).

(D) TIN2 deletion diminishes the telomeric IF signals for TRF1 and TRF2. Method as in (B).

(E) Effect of TIN2 deletion (H&R-Cre) on soluble and chromatin-bound shelterin proteins. Equal cell equivalents of the whole cell lysate (WC), cytoplasmic proteins (CP), nucleoplasmic proteins (NP), and the chromatin-bound fraction (CB) were analyzed. α-tubulin is cytoplasmic.

(F) Immunoblotting for Myc-POT1a and -TPP1 in $TIN2^{F/F}$ MEFs infected with pLPC-puro-Myc-TPP1 or pWZL-Hygro-Myc-POT1a and treated with Cre (92 h) after drug selection.

(G) Telomeric ChIP for Myc-POT1a and -TPP1 before and after TIN2 deletion. ChIP assay with TIN2 Ab (1447) and myc Ab as in (F). Input: 20% of the input DNA.

(H) Quantification of the ChIP signals in (G) after normalization to input and subtraction of background (PI).

(I) Telomeric localization of Myc-TPP1 and -POT1a. IF for myc (red) and telomeric FISH (green) at 92 hr post-Cre.

POT1a was reduced to near background levels when TIN2 was absent (Figures 2G and 2H). The endogenous TPP1 also disappeared from telomeres when TIN2 was deleted (Figure 2C). These data argue that TPP1 and POT1a (and most likely POT1b) require TIN2 for their accumulation at telomeres. Similarly, short hairpin RNA (shRNA)-mediated knockdown of TIN2 resulted in loss of POT1 from human telomeres (Figures S2E–S2G). The TIN2-dependent tethering of TPP1/POT1 to both TRF1 and TRF2, explains why neither TRF1 nor TRF2 knockout cells have the phenotypes typical of the POT1a/b double-knockout mice (DKO) (Sfeir et al., 2009; Celli and de Lange, 2005; Denchi and de Lange, 2007).

TIN2 Deletion Induces the 3′ Overhang Phenotype Typical of POT1b Deficiency

A characteristic phenotype associated with the loss of POT1b or TPP1 from telomeres is an increase in the ss-TTAGGG repeats. Deletion of TIN2 resulted in the same overhang phenotype observed upon deletion of POT1b (Figure 3A). The normalized 3′ overhang signal increased by 2–4-fold within 2 or 4 days after introduction of Cre. In contrast, the pattern of the total telomeric DNA was not overtly affected by deletion of TIN2.

Loss of TIN2 Induces Polyploidization through Endoreduplication

A prominent phenotype of POT1a/b or TPP1 deficiency is the formation of polyploid cells formed through endoreduplication (Hockemeyer et al., 2006; Davoli et al., 2010; Kibe et al., 2010). Similarly, TIN2-deficient cells showed an increase in ploidy, resulting in fluorescence-activated cell sorting (FACS) profiles showing discrete peaks at 8-, 16-, and 32N of DNA content (Figure 3B). Consistent with endoreduplication, TIN2-deficient cells had diplochromosomes (Figure 3C) and showed telomere clustering (Figure 3D). Both phenomena are observed in the POT1a/b DKO cells and are consistent with the persistent association of sister chromatids through multiple rounds of DNA replication.

After Replication, Leading- and Lagging-End Telomeres Fuse in TIN2-Deficient Cells

POT1a/b DKO cells lack the prominent G1-type telomere fusions typical of TRF2-deficient cells. The telomere fusions in POT1a/b DKO cells arise most often after DNA replication, as evidenced by chromatid-type fusions. Importantly, these fusions can involve both products of DNA replication: telomeres duplicated by leading-strand DNA synthesis (leading-end telomeres) and those duplicated by lagging-strand DNA synthesis (lagging-end telomeres). As a consequence, POT1a/b DKO cells display fused sister chromatids which are exceedingly rare in TRF2-deficient cells (Hockemeyer et al., 2006). Sister telomere fusions also occur in TPP1-knockout cells, presumably due to the loss of POT1a/b (Kibe et al., 2010; Tejera et al., 2010).

Metaphase chromosomes from TIN2-deficient cells were examined using chromosome-orientation fluorescence in situ (CO-FISH) to identify leading- and lagging-end telomeres (Figures 3E and 3F). TIN2 deletion induced a significant level of telomere fusions. A substantial fraction of the fusions were generated after DNA replication because they involved the fusion of duplicated chromatids (Figures 3E and 3F). Among these, sister telomere fusions were prominent, indicating that TIN2 loss resulted in deprotection of both leading- and lagging-end telomeres. Leading-to-lagging end fusions were also noted among the chromatid-type fusions between two different chromosomes (Figure 3E).

TIN2 deletion also resulted in chromosome-type fusions, which could indicate either a fusion in G1 or result from duplication of the chromatid-type fusions formed in the preceding G2. As shown below, the chromosome-type fusions in the TIN2 knockout cells are most likely the result of diminished loading of TRF2.

There was no prominent loss of the telomeric signals after TIN2 deletion, the telomeres did not show the fragile-site phenotype associated with TRF1 loss, and telomeric DNA containing double-minute chromosomes (TDMs) were not induced (Figure 3E). TIN2 deficiency led to a modest increase in the rate of telomere sister chromatid exchanges (T-SCEs) (~5% compared to 0.5% in the control) but the statistical significance of this phenotype is marginal ($p = 0.06$, Student's t test; Figures 3E and 3F).

Activation of ATR and ATM at Telomeres Lacking TIN2

As expected, TIN2 deletion resulted in the activation of a DNA damage response, which was evident from the accumulation of 53BP1 at telomeres, the proliferative arrest, and phosphorylation of Chk1 and Chk2 (Figures 4A and 4B; Figure S2). Exogenous TIN2 repressed the accumulation of 53BP1 at the telomeres of TIN2 KO cells, whereas expression of Myc-TPP1 or Myc-POT1a had no effect (Figures S3A and S3B). Compound TIN2/ATR and TIN2/ATM double knockout cells indicated that the DNA damage response involved both the ATM and the ATR kinases (Figures 4 and S3C–S3E). This contrasts with the specific induction of either ATM or ATR signaling upon individual deletion of other shelterin components. The ATR response was evident from the phosphorylation of Chk1, which was absent when TIN2 and ATR were codeleted from $TIN2^{F/F}ATR^{F/F}$ cells (Figure 4B). Furthermore, deletion of TIN2 resulted in significantly fewer TIFs per nucleus when ATR was absent (Figures 4A and 4C). The DNA damage response elicited by TIN2 loss also involved the ATM kinase, as shown by phosphorylation of Chk2, which was diminished when ATM was absent, and a reduced TIF response in ATM-deficient cells (Figures 4B and 4C). Consistent with signaling involving both ATM and ATR, the inhibition of both kinases with caffeine lowered the frequency of telomere dysfunction-induced foci (TIFs) more than the absence of either kinase alone (Figure S3F). In contrast, the absence of DNA-dependent protein kinase, catalytic subunits (DNA-PKcs) did not affect the DNA damage response at telomeres lacking TIN2 (Figure S3G).

RPA at Telomeres and RPA-Coated Chromatin Bridges after TIN2 Loss

TIN2 loss also recapitulates the phenotype of POT1a/b deletion with regard to the association of RPA with telomeres. Accumulation of RPA at telomeres was previously observed 4 h after removal of POT1a from POT1b-deficient cells (Gong and de Lange, 2010). Approximately 15% of the TIN2-deficient cells

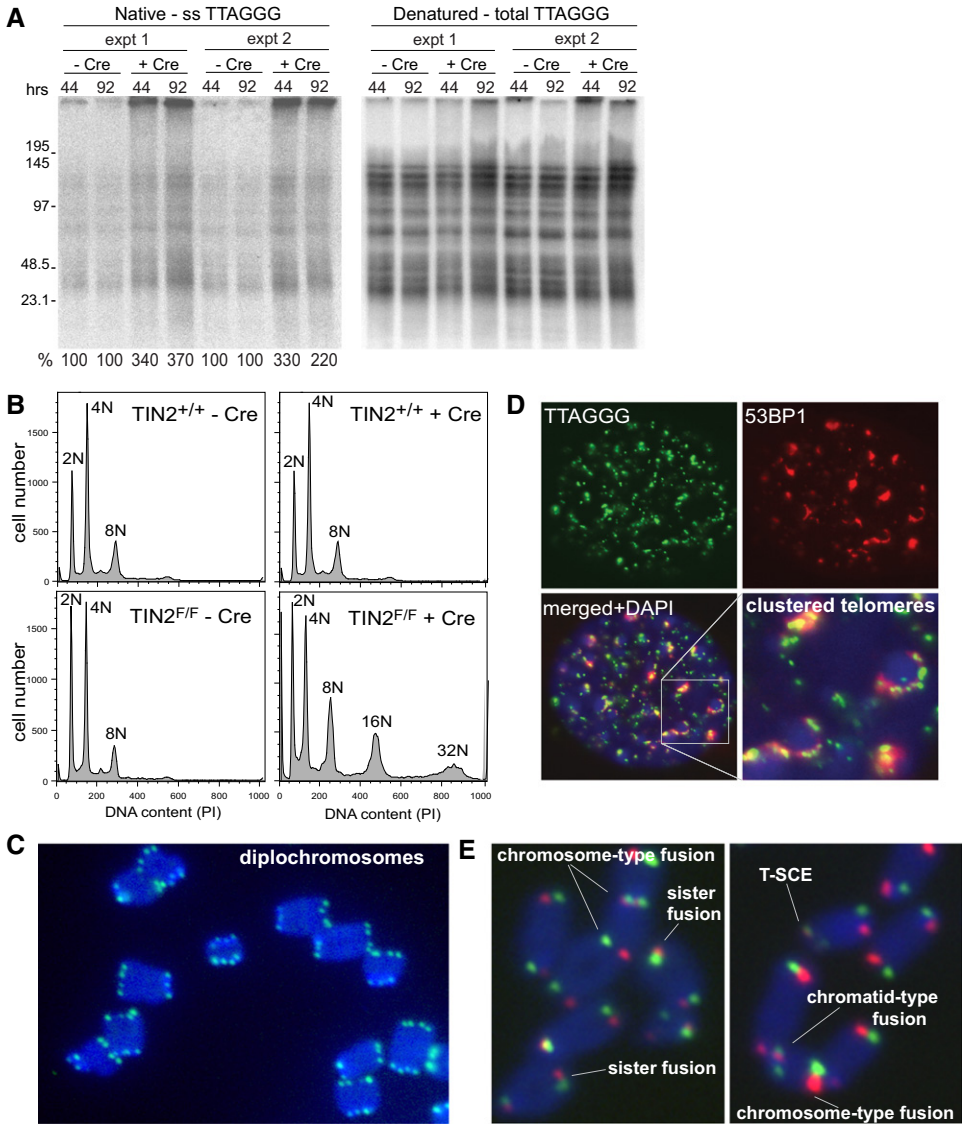

F

	Telomere fusions (% of telomeres)			
	Chromosome-type	Chromatid-type	Sister	T-SCEs
$TIN2^{F/F}$ -Cre	<0.1%	<0.1%	<0.1%	0.5±0.6%
$TIN2^{F/F}$ +Cre	15.8±2.6%	2.8±1.1%	8.2±2.5%	3.7±2.2%

Figure 3. Excess Short-Stranded Telomeric DNA, Endoreduplication, and Telomere Fusions in TIN2 Knockout Mice

(A) In-gel hybridization assay for ss telomeric DNA after TIN2 deletion. Left: TelC signals under the native condition. Right: same gel re-hybridized after in situ denaturation of the DNA. Overhang signals (left) were normalized to the total telomeric signals (right) and compared to $TIN2^{F/F}$ MEFs without Cre. Two independent experiments are shown.

(B) FACS analysis for DNA content (propidium iodide) of $TIN2^{F/F}$ and $TIN2^{+/+}$ MEFs after pWZL-Cre infection (day 8). Both MEFs contained tetraploid cells prior to deletion of TIN2.

(C) Diplochromosomes in Cre-treated $TIN2^{F/F}$ MEFs. DNA stained with DAPI (blue) and telomeric FISH (green).

(D) Telomere clustering in a polyploid TIN2-deficient cell. Staining for 53BP1 IF (red) and telomeric FISH (green). DNA is stained with DAPI (blue). The enlarged image illustrates clustered telomeres.

(E) CO-FISH illustrating examples of telomere fusions and T-SCEs in metaphases of TIN2-deficient cells. Red: leading-end telomeres; green: lagging-end telomeres; blue: DAPI DNA stain.

(F) Summary of telomere phenotypes induced by TIN2 deletion determined by CO-FISH as shown in (E). Values are averages of 3-4 independent experiments (1000-2000 telomeres/experiment) and SDs. Sister fusions were scored on long arm telomeres in metaphase spreads with separated chromosome arms.

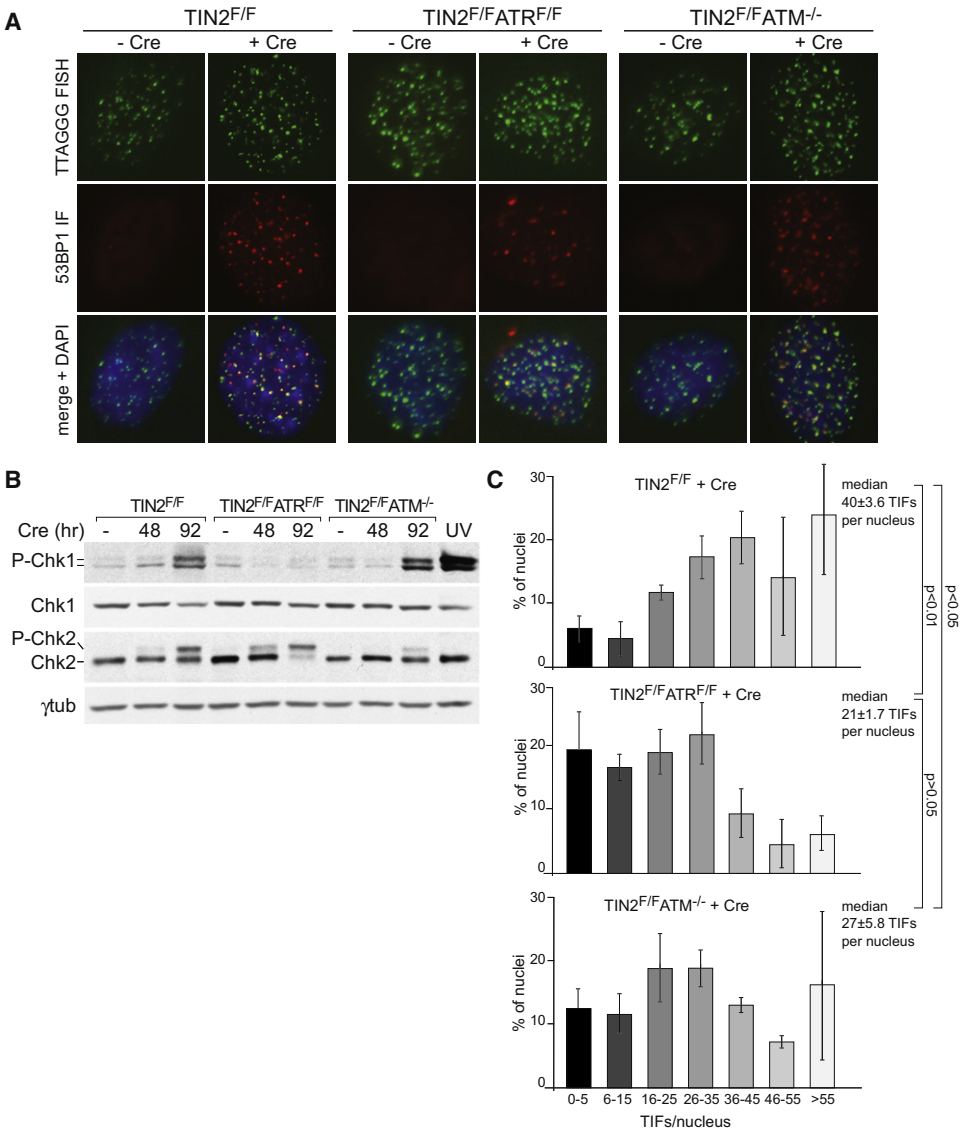

Figure 4. TIN2 Loss Induces ATM and ATR Signaling

(A) TIFs detected by immunofluorescent FISH in MEFs of the indicated genotypes. MEFs were fixed at 92 hr after H&R Cre and processed as in Figure 3D.

(B) Immunoblots of phospho-Chk1, total Chk1, and Chk2 in MEFs of the indicated genotypes at 48 and 92 hr after H&R Cre. UV treated (30 min after 25 J/m^2) TIN2$^{F/F}$ MEFs serve as a control.

(C) Quantification of the effect of ATM and ATR deletion on TIFs induced by TIN2 deletion. TIN2$^{F/F}$ (top), TIN2$^{F/F}$ATR$^{F/F}$ (middle), and TIN2$^{F/F}$ATM$^{-/-}$ MEFs (bottom) were scored for 53BP1 TIFs per nucleus (n > 100) after H&R-Cre (92 h). Averages of three independent experiments and SDs. P values from one-way analysis of variance (ANOVA) and Bonferroni's multiple comparison test.

showed RPA foci at telomeres, whereas RPA was not observed at telomeres in TIN2-proficient cells (Figure 5A). The presence of RPA at telomeres was noteworthy because the cells were not in S phase, as surmised from the generally low level of RPA staining at nontelomeric loci. After POT1a deprivation, RPA also becomes detectable at telomeres in nonreplicating cells, although to a lesser extent than in S phase (Gong and de Lange, 2010). Approximately 40% of the POT1a-deprived G1 cells showed five or more RPA foci that were inferred to be at dysfunctional telomeres, based on their colocalization with 53BP1 (Gong and de Lange, 2010). Thus, the level of RPA accumulation at nonreplicating telomeres is lower after TIN2 loss compared to POT1a removal. This difference may be due to timing differences in the two methods because Cre-mediated deletion of TIN2 required several days before analysis, whereas POT1a loss was studied with a rapidly acting degron fusion. Nonetheless, this data establish that RPA can associate with telomeres after TIN2 removal.

We noticed that RPA often stained the chromatin bridges that connect individual nuclei (Figure S4). Chromatin bridges occur in

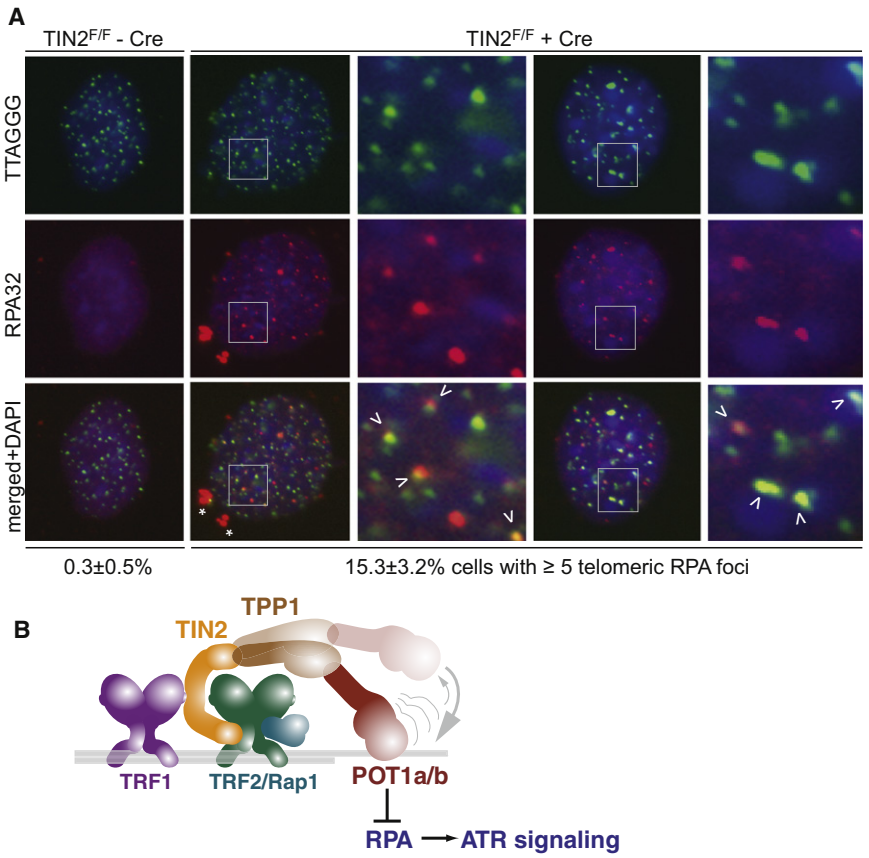

Figure 5. RPA at Telomeres after TIN2 Deletion

(A) Colocalization of RPA with telomeres in TIN2$^{F/F}$ MEFs infected with Cre (92 h). RPA32 IF (red) and telomeric DNA FISH (green). Arrowheads: RPA signals at telomeres. Below: quantification of cells with five or more telomeric RPA signals as averages from three experiments ($n \geq 100$ nuclei) and standard errors. Asterisks: micronuclei. The cells used also expressed Myc-RPA32 but the myc-tag was not used for immunofluorescence.

(B) Model for RPA exclusion through TIN2-tethered TPP1/POT1. POT1 is shown to have a greater on rate (arrow) due to its TPP1 connection to the TIN2/TRF1/TRF2 complex on the duplex telomeric DNA. Although only the most terminal shelterin complex is depicted, POT1 in shelterin distal from the telomere terminus may well be physically close to ssDNA due to higher order structure of the telomeric DNA. Tethered POT1 may also prevent RPA binding to the ss telomeric DNA in the D-loop when telomeres are in the t-loop configuration (data not shown).

immortalized MEFs experiencing telomere fusions and might represent stretched chromatin from fused chromosomes that persist through cytokinesis. Alternatively, they could represent unresolved recombination events, but T-SCEs are infrequent in the TIN2-knockout setting. The presence of RPA indicates that at least part of this DNA is single-stranded. Most of the RPA bridges also showed telomeric FISH signals that were consistent with their derivation from dysfunctional telomeres (Figure S4). We also noted very prominent RPA signals on the micronuclei that often form in mouse embryonic fibroblasts (MEFs) experiencing telomere dysfunction (Figure 5A), suggesting extensive DNA processing in these compartments.

Collectively, the data on the TIN2-deficient cells reveal a key role for TIN2 in facilitating telomere protection by POT1a/b (Figure 5B).

TIN2 Contributes to TRF2-Mediated Repression of ATM Signaling

The activation of the ATM kinase pathway and the formation of chromosome-type fusions suggested diminished TRF2 function in the TIN2 knockout cells. We used two approaches to determine whether these phenotypes resulted from reduced association of TRF2 with telomeres or were due to the absence of TIN2 from telomere-bound TRF2. In the first approach, Myc-tagged TRF2 was overexpressed in TIN2$^{F/F}$ MEFs to determine whether an increased level of TRF2 expression could ameliorate these phenotypes (Figures 6A–6C). In the second approach, we complemented conditional TRF2 knockout cells with an allele of mouse TRF2 lacking amino acids 350–365, which is the predicted TIN2 interaction motif (Chen et al., 2008) (Figures 6D–6H). This deletion mutant, TRF2$^{\Delta T}$, binds to telomeres and recruits Rap1 but lacks the ability to interact with TIN2 based on a far-western assay (Figures 6D, S5A, and S5B). Consistent with previous telomeric ChIP of TIN2 and TRF1 in TRF2 knockout cells (Hockemeyer et al., 2007), cells expressing TRF2$^{\Delta T}$ show diminished accumulation of TIN2 at telomeres, whereas TRF1 appears largely unaffected (Figure S5B).

As expected, the telomeric overhang phenotype associated with TIN2 deletion was unaltered upon overexpression of TRF2, and no increase in the telomeric overhang occurred in a clonal line expressing TRF2$^{\Delta T}$ rather than wild-type TRF2 (Figures 6C and 6E). Furthermore, Chk1 phosphorylation was induced after TIN2 loss despite the overexpression of TRF2 (Figure 6B). These results are consistent with the requirement for TIN2 in the tethering of TPP1/POT1a/b and they argue against a role for TRF2 in the recruitment of POT1a/b, as had been proposed for human POT1 (Yang et al., 2005).

TIN2-deficient MEFs with overexpressed TRF2 showed a strong reduction in chromosome-type telomere fusions as determined in metaphase spreads (Figure 6A). In addition, the TRF2$^{\Delta T}$ allele repressed the occurrence of telomere fusion products in gel electrophoresis analysis of telomeric restriction fragments of TRF2$^{F/-}$ cells treated with Cre (Figure 6E). Thus, the ability of TRF2 to repress nonhomologous end-joining (NHEJ) of telomeres does not require interaction with TIN2.

However, we observed an intermediate effect regarding the contribution of TIN2 to the repression of ATM signaling by TRF2. The phosphorylation of Chk2 in TIN2 KO cells overexpressing wild-type TRF2 and in TRF2-knockout cells containing

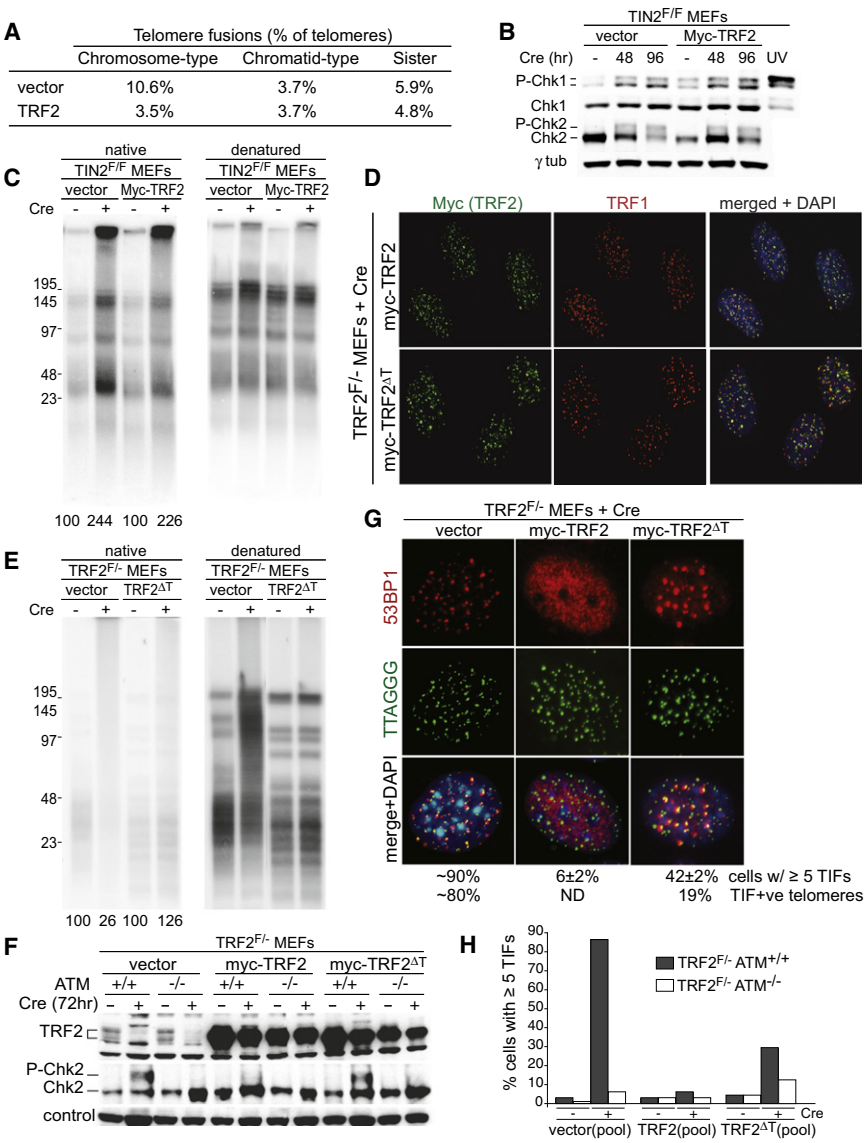

Figure 6. TRF2 Requires TIN2 for Repression of ATM But Not NHEJ

(A) Overexpression of TRF2 reduces chromosome-type fusions in TIN2 knockout cells. Telomere fusions were scored as in Figures 3E and 3F.

(B) Immunoblots for Chk1 and Chk2 phosphorylation. Cells as in (A) and processing as in Figure 4B.

(C) No effect of TRF2 overexpression on telomeric overhang in TIN2 knockout cells. Cells as in (A) and processing and quantification as in Figure 3A.

(D) Telomeric localization of the TRF2$^{\Delta T}$ mutant. TRF2$^{F/-}$ MEFs were infected with the indicated TRF2 alleles, selected, cloned, and treated with Cre. TRF2 was detected with the Myc Ab in combination with immunofluoresence for TRF1.

(E) Repression of telomere fusions by TRF2$^{\Delta T}$. Cells as in D were analyzed at 120 hr post-Cre as in Figure 3A.

(F) Chk2 phosphorylation in TRF2$^{\Delta T}$ cells. TRF2$^{F/-}$ATM$^{+/+}$ and TRF2$^{F/-}$ATM$^{-/-}$ cells were infected with the indicated retroviruses, selected, and treated with Cre as indicated. Immunblotting for Chk2 and TRF2 at 72 h post-Cre. Loading control: nonspecific band in the Chk2 blot.

(G) TIFs in TRF2$^{\Delta T}$ cells. The indicated clonal lines (as in (D) were treated with Cre (96 h) and analyzed for TIFs as in Figure 4A. Note fewer but larger 53BP1 TIFs in TRF2$^{\Delta T}$ cells.

(H) Quantification of the TIF response in the indicated cells at 96 h after Cre. Pools of TRF2$^{F/-}$ATM$^{+/+}$ and TRF2$^{F/-}$ATM$^{-/-}$ infected as indicated were used for TIF assays as in Figure 4A.

the TRF2$^{\Delta T}$ allele was only slightly reduced (Figures 6B–6F). Furthermore, TRF2$^{\Delta T}$ did not fully repress TIF formation in TRF2-knockout cells (Figures 6G and 6H). Thus, the interaction of TRF2 with TIN2 appears to improve TRF2's ability to repress ATM kinase signaling but has no effect on its protection of telomeres from NHEJ.

DISCUSSION

The Role of TIN2 within Shelterin

This characterization of the telomere defects in TIN2-deficient cells completes the catalog of telomere dysfunction phenotypes associated with loss of individual shelterin components (Table 1). Each shelterin subunit is unique with regard to the spectrum of aberrant events at chromosome ends elicited upon its loss. This phenotypic diversity bears witness to the functional compartmentalization within shelterin.

Importantly, TIN2 deletion mimics the loss of TPP1 or POT1a/b in inducing the same combination of phenotypes: the activation of ATR signaling, endoreduplication, postreplicative telomere fusion involving both leading- and lagging-end telomeres, and the induction of excessive single-stranded TTAGGG repeat DNA (Table 1). Therefore, it appears evident that TIN2, like TPP1, is required to allow the POT1 proteins to fulfill their functions.

In addition to the phenotypes typical of POT1a/b loss, TIN2-deficient cells show ATM kinase signaling and a modest level of chromosome-type telomere fusions, which are phenotypes ascribed to TRF2 loss (Table 1). Our data argue that the chromosome-type telomere fusions are due to the diminished loading of TRF2 on telomeres lacking TIN2, rather than a genuine contribution of TIN2 to this function of TRF2. In contrast, we find that TRF2 relies on its association with TIN2 for maximal repression of the ATM kinase pathway. None of the other shelterin components, including the TRF2-binding partner, Rap1, appear to contribute to the repression of ATM signaling by TRF2.

In contrast to this contribution of TIN2 to the function of TRF2, TIN2 deletion does not show the fragile telomere phenotype associated with the telomeric replication problems resulting

Table 1. Phenotypes Associated with the Deletion of Individual Shelterin Components

		DDR			Telomere Fusions					
						Chromatid-Type				
Gene	Viable	ATR	ATM	Endoreduplication	Chromosome-Type	Leading	Lagging	3′ Overhang	Fragile Telomeres	T-SCEs (in Ku Null)
POT1a	–	+	–	+	+	+	+	–	–	–
POT1b	+	–	–	–	–	–	–	+	–	–
POT1a/b	–	++	–	++	+	+	+	+	–	+
TPP1	–	++	–	++	+	+	+	+	–	?
TIN2	–	++	+	++	+	+	+	+	–	?
TRF1	–	+[a]	–	+	–	–	–	–	+	?
TRF2	–	–	++	+	++	+[b]	–	–	–	+
Rap1	+	–	–	–	–	–	–	–	–	+

[a] ATR signaling requires progression through S phase.
[b] Leading-end chromatid fusions occur only in absence of MRN or ATM.

from loss of TRF1 (Martinez et al., 2010; Sfeir et al., 2010). Thus, the lowered amount of TRF1 on telomeres lacking TIN2 (Figure 2) is likely sufficient for efficient replication of the telomeric repeat array. Previous work using either a TRF1 dominant-negative allele or tankyrase to remove TRF1 also showed that TRF1 levels can be reduced substantially without the induction of deleterious telomeric phenotypes (Karlseder et al., 2002; van Steensel and de Lange, 1997; Smith and de Lange, 2000).

In sum, the TIN2-tether is required for all the protective functions of the TPP1/POT1a/b complexes, and the binding of TIN2 to TRF2 contributes to the ability of TRF2 to repress ATM signaling. In contrast, although TRF1 is stabilized on telomeres by TIN2, the telomere-bound TRF1 operates independently of its association with TIN2.

RPA Exclusion and Repression of ATR Signaling by TPP1/POT1

Zou and colleagues raised the possibility that TPP1/POT1 are assisted by hnRNPA1, which, unlike TPP1/POT1, has the ability to remove RPA from single-stranded telomeric DNA in vitro (Flynn et al., 2011). The subsequent displacement of hnRNPA1 by POT1 is proposed to require recruitment of hnRNPA1 to TERRA RNA, which provides optimal binding sites for hnRNPA1 but not for POT1 (Nandakumar et al., 2010). It was further proposed that the stepwise removal of RPA by hnRNPA1 and hnRNPA1 by TERRA is orchestrated by variation in TERRA levels during S phase such that the replicated telomeres end up bound by POT1 rather than RPA or hnRNPA1. However, this model does not explain why POT1, once loaded at the end of S phase, is not displaced by RPA. POT1 also does not show the predicted increase on telomeres at the end of S phase and in G2 (Verdun et al., 2005). Finally, the hnRNPA1/TERRA model for RPA competition predicts that the dependence on POT1 should be greater in G2 and G1 than in most of S phase, when RPA is repressed by hnRNPA1. Yet, removal of POT1 from telomeres initiates an RPA-dependent ATR signaling within a few hours, regardless of whether the cells are in S, G2, or G1 phase (Gong and de Lange, 2010). Thus, while hnRNPs may well play a role in the protection of telomeres, it is likely that other mechanisms are required to exclude RPA from the single-stranded telomeric DNA.

We propose that TPP1/POT1 acts as an effective competitor for RPA when bound to TIN2 (Figure 5B). The crux of the TIN2-tether model for POT1 function is that, through its association with TIN2, the TPP1/POT1 heterodimer has two binding sites at chromosome ends, one on the ssDNA and one on a nearby TIN2/TRF1/TRF2 complex. This dual binding will increase the on rate of POT1 binding to the ssTTAGGG repeats and, thereby, greatly enhance the stability of the TPP1/POT1 complex on the ssDNA.

We envisage that TPP1/POT1 heterodimers are associated with TIN2 that is bound to the TRF1/TRF2 units anywhere on the duplex telomeric repeat array. This view is in agreement with ChIP data and also with the ability of POT1 to accumulate on telomeres independent of its ssDNA-binding activity (Loayza and de Lange, 2003). As TIN2/TRF1/TRF2 are more abundant than TPP1/POT1 (Takai et al., 2010), there is ample TIN2 for the binding of all TPP1/POT1. Most of the tethered POT1 is not likely to be positioned adjacent to the ss telomeric DNA. However, POT1 at a distal site may well be in close proximity to, and interact with, the ss telomeric DNA owing to a higher order structure of the telomeric chromatin. When telomeres are in the t-loop configuration, the ssDNA in the D-loop is also likely to require engagement of POT1 to prevent ATR signaling. In this setting, POT1 tethered to the shelterin on the duplex DNA formed by strand invasion of the 3′ overhang will be positioned to engage the ssDNA in the D-loop. Further in vitro tests will provide insight into the validity of the TIN2-tethering model for RPA exclusion by TPP1/POT1.

EXPERIMENTAL PROCEDURES

Analysis of the Abundance and Biochemical Features of RPA and TPP1/POT1a

Flag-human POT1, His_6-mouse POT1a, His_6-mouse POT1b, and Flag-mouse TPP1 were purified from baculovirus-infected cells as described (Palm et al., 2009; Takai et al., 2010). Recombinant human RPA was isolated as described (Binz et al., 2006), with minor modifications. Probe-labeling reactions and gel shift assays were performed as described (Palm et al., 2009), with minor modification. For additional information, see Supplemental Information.

Tinf2 Gene Targeting, Mouse Strains, and Generation of Mouse Embryonic Fibroblasts

The targeting construct was constructed from a bacterial artificial chromosome (BAC; [Children's Hospital Oakland Research Institute]) using the recombineering method. Targeted embryonic stem cell clones from albino C57BL/6J mice were screened by genomic blotting of BglI-digested DNA and injected into C57BL/6J blastcysts. Mice carrying the TIN2 Flox allele were generated using the FLPe deleter strain (The Jackson Laboratory). Additional information is available in Supplemental Information.

Analysis of Shelterin Components and Telomere (Dys)function

Detailed experimental procedures are available in Supplemental Information. Immunoblotting for shelterin and cell fractionation was performed as described previously (Takai et al., 2010). Telomeric DNA FISH was combined with immunofluorescence as described previously (Denchi and de Lange, 2007). For RPA, the in situ cell fractionation protocol of Mirzoeva and Petrini was used (Mirzoeva and Petrini, 2001). ChIP was performed as described (Loayza and de Lange, 2003), with minor modification. Telomeric overhang signals and telomeric restriction fragment patterns were analyzed by in-gel analysis as previously described (Celli and de Lange, 2005). The procedures for telomeric FISH and CO-FISH on metaphase spreads were as described (Sfeir et al., 2009).

SUPPLEMENTAL INFORMATION

Supplemental Information includes five figures, Supplemental Experimental Procedures, and Supplemental References and can be found with this article online at doi:10.1016/j.molcel.2011.08.043.

ACKNOWLEDGMENTS

We thank Devon White for expert mouse husbandry and the Rockefeller University transgenics facility for help with generating mouse strains. We thank Marc Wold for the RPA expression plasmid and Yihu Xie and Nikola Pavletich for the gel filtration analysis of TPP1/POT1a. Members of the de Lange laboratory are thanked for advice and comments. This work was supported by a postdoctoral fellowship from the American Cancer Society to D.F., a postdoctoral fellowship from the Japan Society for the Promotion of Science and the Toyobo Biotechnology Foundation to T.K., and grants (AG016642 and GM49046) from the NIH to T.d.L. T.d.L. is an American Cancer Society Research Professor.

Received: March 29, 2011
Revised: July 6, 2011
Accepted: August 30, 2011
Published: November 17, 2011

REFERENCES

Abreu, E., Aritonovska, E., Reichenbach, P., Cristofari, G., Culp, B., Terns, R.M., Lingner, J., and Terns, M.P. (2010). TIN2-tethered TPP1 recruits human telomerase to telomeres in vivo. Mol. Cell. Biol. *30*, 2971–2982.

Arnoult, N., Saintome, C., Ourliac-Garnier, I., Riou, J.F., and Londoño-Vallejo, A. (2009). Human POT1 is required for efficient telomere C-rich strand replication in the absence of WRN. Genes Dev. *23*, 2915–2924.

Ball, H.L., Myers, J.S., and Cortez, D. (2005). ATRIP binding to replication protein A-single-stranded DNA promotes ATR-ATRIP localization but is dispensable for Chk1 phosphorylation. Mol. Biol. Cell *16*, 2372–2381.

Ball, H.L., Ehrhardt, M.R., Mordes, D.A., Glick, G.G., Chazin, W.J., and Cortez, D. (2007). Function of a conserved checkpoint recruitment domain in ATRIP proteins. Mol. Cell. Biol. *27*, 3367–3377.

Baumann, P., and Price, C. (2010). Pot1 and telomere maintenance. FEBS Lett. *584*, 3779–3784.

Binz, S.K., Dickson, A.M., Haring, S.J., and Wold, M.S. (2006). Functional assays for replication protein A (RPA). Methods Enzymol. *409*, 11–38.

Blackwell, L.J., and Borowiec, J.A. (1994). Human replication protein A binds single-stranded DNA in two distinct complexes. Mol. Cell. Biol. *14*, 3993–4001.

Blackwell, L.J., Borowiec, J.A., and Mastrangelo, I.A. (1996). Single-stranded-DNA binding alters human replication protein A structure and facilitates interaction with DNA-dependent protein kinase. Mol. Cell. Biol. *16*, 4798–4807.

Celli, G.B., and de Lange, T. (2005). DNA processing is not required for ATM-mediated telomere damage response after TRF2 deletion. Nat. Cell Biol. *7*, 712–718.

Chai, W., Du, Q., Shay, J.W., and Wright, W.E. (2006). Human telomeres have different overhang sizes at leading versus lagging strands. Mol. Cell *21*, 427–435.

Chen, Y., Yang, Y., van Overbeek, M., Donigian, J.R., Baciu, P., de Lange, T., and Lei, M. (2008). A shared docking motif in TRF1 and TRF2 used for differential recruitment of telomeric proteins. Science *319*, 1092–1096.

Chiang, Y.J., Kim, S.H., Tessarollo, L., Campisi, J., and Hodes, R.J. (2004). Telomere-associated protein TIN2 is essential for early embryonic development through a telomerase-independent pathway. Mol. Cell. Biol. *24*, 6631–6634.

Cimprich, K.A., and Cortez, D. (2008). ATR: an essential regulator of genome integrity. Nat. Rev. Mol. Cell Biol. *9*, 616–627.

Davoli, T., Denchi, E.L., and de Lange, T. (2010). Persistent telomere damage induces bypass of mitosis and tetraploidy. Cell *141*, 81–93.

Denchi, E.L., and de Lange, T. (2007). Protection of telomeres through independent control of ATM and ATR by TRF2 and POT1. Nature *448*, 1068–1071.

Flynn, R.L., Centore, R.C., O'Sullivan, R.J., Rai, R., Tse, A., Songyang, Z., Chang, S., Karlseder, J., and Zou, L. (2011). TERRA and hnRNPA1 orchestrate an RPA-to-POT1 switch on telomeric single-stranded DNA. Nature *471*, 532–536.

Giraud-Panis, M.J., Teixeira, M.T., Géli, V., and Gilson, E. (2010). CST meets shelterin to keep telomeres in check. Mol. Cell *39*, 665–676.

Gong, Y., and de Lange, T. (2010). A Shld1-controlled POT1a provides support for repression of ATR signaling at telomeres through RPA exclusion. Mol. Cell *40*, 377–387.

Griffith, J.D., Comeau, L., Rosenfield, S., Stansel, R.M., Bianchi, A., Moss, H., and de Lange, T. (1999). Mammalian telomeres end in a large duplex loop. Cell *97*, 503–514.

He, H., Multani, A.S., Cosme-Blanco, W., Tahara, H., Ma, J., Pathak, S., Deng, Y., and Chang, S. (2006). POT1b protects telomeres from end-to-end chromosomal fusions and aberrant homologous recombination. EMBO J. *25*, 5180–5190.

Hockemeyer, D., Daniels, J.P., Takai, H., and de Lange, T. (2006). Recent expansion of the telomeric complex in rodents: Two distinct POT1 proteins protect mouse telomeres. Cell *126*, 63–77.

Hockemeyer, D., Palm, W., Else, T., Daniels, J.P., Takai, K.K., Ye, J.Z., Keegan, C.E., de Lange, T., and Hammer, G.D. (2007). Telomere protection by mammalian Pot1 requires interaction with Tpp1. Nat. Struct. Mol. Biol. *14*, 754–761.

Hockemeyer, D., Palm, W., Wang, R.C., Couto, S.S., and de Lange, T. (2008). Engineered telomere degradation models dyskeratosis congenita. Genes Dev. *22*, 1773–1785.

Houghtaling, B.R., Cuttonaro, L., Chang, W., and Smith, S. (2004). A dynamic molecular link between the telomere length regulator TRF1 and the chromosome end protector TRF2. Curr. Biol. *14*, 1621–1631.

Karlseder, J., Smogorzewska, A., and de Lange, T. (2002). Senescence induced by altered telomere state, not telomere loss. Science *295*, 2446–2449.

Kenny, M.K., Schlegel, U., Furneaux, H., and Hurwitz, J. (1990). The role of human single-stranded DNA binding protein and its individual subunits in simian virus 40 DNA replication. J. Biol. Chem. *265*, 7693–7700.

Kibe, T., Osawa, G.A., Keegan, C.E., and de Lange, T. (2010). Telomere protection by TPP1 is mediated by POT1a and POT1b. Mol. Cell. Biol. *30*, 1059–1066.

Kim, C., Snyder, R.O., and Wold, M.S. (1992). Binding properties of replication protein A from human and yeast cells. Mol. Cell. Biol. *12*, 3050–3059.

Kim, C., Paulus, B.F., and Wold, M.S. (1994). Interactions of human replication protein A with oligonucleotides. Biochemistry *33*, 14197–14206.

Kim, S.H., Kaminker, P., and Campisi, J. (1999). TIN2, a new regulator of telomere length in human cells. Nat. Genet. *23*, 405–412.

Kim, S.H., Beausejour, C., Davalos, A.R., Kaminker, P., Heo, S.J., and Campisi, J. (2004). TIN2 mediates functions of TRF2 at human telomeres. J. Biol. Chem. *279*, 43799–43804.

Kumagai, A., Kim, S.M., and Dunphy, W.G. (2004). Claspin and the activated form of ATR-ATRIP collaborate in the activation of Chk1. J. Biol. Chem. *279*, 49599–49608.

Lavrik, O.I., Kolpashchikov, D.M., Weisshart, K., Nasheuer, H.P., Khodyreva, S.N., and Favre, A. (1999). RPA subunit arrangement near the 3′-end of the primer is modulated by the length of the template strand and cooperative protein interactions. Nucleic Acids Res. *27*, 4235–4240.

Lei, M., Podell, E.R., and Cech, T.R. (2004). Structure of human POT1 bound to telomeric single-stranded DNA provides a model for chromosome end-protection. Nat. Struct. Mol. Biol. *11*, 1223–1229.

Liu, D., O'Connor, M.S., Qin, J., and Songyang, Z. (2004a). Telosome, a mammalian telomere-associated complex formed by multiple telomeric proteins. J. Biol. Chem. *279*, 51338–51342.

Liu, D., Safari, A., O'Connor, M.S., Chan, D.W., Laegeler, A., Qin, J., and Songyang, Z. (2004b). PTOP interacts with POT1 and regulates its localization to telomeres. Nat. Cell Biol. *6*, 673–680.

Loayza, D., and De Lange, T. (2003). POT1 as a terminal transducer of TRF1 telomere length control. Nature *423*, 1013–1018.

Loayza, D., Parsons, H., Donigian, J., Hoke, K., and de Lange, T. (2004). DNA binding features of human POT1: a nonamer 5′-TAGGGTTAG-3′ minimal binding site, sequence specificity, and internal binding to multimeric sites. J. Biol. Chem. *279*, 13241–13248.

MacDougall, C.A., Byun, T.S., Van, C., Yee, M.C., and Cimprich, K.A. (2007). The structural determinants of checkpoint activation. Genes Dev. *21*, 898–903.

Makarov, V.L., Hirose, Y., and Langmore, J.P. (1997). Long G tails at both ends of human chromosomes suggest a C strand degradation mechanism for telomere shortening. Cell *88*, 657–666.

Martinez, P., Thanasoula, M., Carlos, A.R., Gómez-López, G., Tejera, A.M., Schoeftner, S., Dominguez, O., Pisano, D.G., Tarsounas, M., and Blasco, M.A. (2010). Mammalian Rap1 controls telomere function and gene expression through binding to telomeric and extratelomeric sites. Nat. Cell Biol. *12*, 768–780.

McElligott, R., and Wellinger, R.J. (1997). The terminal DNA structure of mammalian chromosomes. EMBO J. *16*, 3705–3714.

Miyake, Y., Nakamura, M., Nabetani, A., Shimamura, S., Tamura, M., Yonehara, S., Saito, M., and Ishikawa, F. (2009). RPA-like mammalian Ctc1-Stn1-Ten1 complex binds to single-stranded DNA and protects telomeres independently of the Pot1 pathway. Mol. Cell *36*, 193–206.

Mirzoeva, O.K., and Petrini, J.H. (2001). DNA damage-dependent nuclear dynamics of the Mre11 complex. Mol Cell Biol *21*, 281–288.

Namiki, Y., and Zou, L. (2006). ATRIP associates with replication protein A-coated ssDNA through multiple interactions. Proc. Natl. Acad. Sci. USA *103*, 580–585.

Nandakumar, J., Podell, E.R., and Cech, T.R. (2010). How telomeric protein POT1 avoids RNA to achieve specificity for single-stranded DNA. Proc. Natl. Acad. Sci. USA *107*, 651–656.

O'Connor, M.S., Safari, A., Xin, H., Liu, D., and Songyang, Z. (2006). A critical role for TPP1 and TIN2 interaction in high-order telomeric complex assembly. Proc. Natl. Acad. Sci. USA *103*, 11874–11879.

Palm, W., and de Lange, T. (2008). How shelterin protects mammalian telomeres. Annu. Rev. Genet. *42*, 301–334.

Palm, W., Hockemeyer, D., Kibe, T., and de Lange, T. (2009). Functional dissection of human and mouse POT1 proteins. Mol. Cell. Biol. *29*, 471–482.

Savage, S.A., Giri, N., Baerlocher, G.M., Orr, N., Lansdorp, P.M., and Alter, B.P. (2008). TINF2, a component of the shelterin telomere protection complex, is mutated in dyskeratosis congenita. Am. J. Hum. Genet. *82*, 501–509.

Seroussi, E., and Lavi, S. (1993). Replication protein A is the major single-stranded DNA binding protein detected in mammalian cell extracts by gel retardation assays and UV cross-linking of long and short single-stranded DNA molecules. J. Biol. Chem. *268*, 7147–7154.

Sfeir, A., Kosiyatrakul, S.T., Hockemeyer, D., MacRae, S.L., Karlseder, J., Schildkraut, C.L., and de Lange, T. (2009). Mammalian telomeres resemble fragile sites and require TRF1 for efficient replication. Cell *138*, 90–103.

Sfeir, A., Kabir, S., van Overbeek, M., Celli, G.B., and de Lange, T. (2010). Loss of Rap1 induces telomere recombination in the absence of NHEJ or a DNA damage signal. Science *327*, 1657–1661.

Sibenaller, Z.A., Sorensen, B.R., and Wold, M.S. (1998). The 32- and 14-kilodalton subunits of replication protein A are responsible for species-specific interactions with single-stranded DNA. Biochemistry *37*, 12496–12506.

Smith, S., and de Lange, T. (2000). Tankyrase promotes telomere elongation in human cells. Curr. Biol. *10*, 1299–1302.

Takai, K.K., Hooper, S., Blackwood, S., Gandhi, R., and de Lange, T. (2010). In vivo stoichiometry of shelterin components. J. Biol. Chem. *285*, 1457–1467.

Tejera, A.M., Stagno d'Alcontres, M., Thanasoula, M., Marion, R.M., Martinez, P., Liao, C., Flores, J.M., Tarsounas, M., and Blasco, M.A. (2010). TPP1 is required for TERT recruitment, telomere elongation during nuclear reprogramming, and normal skin development in mice. Dev. Cell *18*, 775–789.

Tsangaris, E., Adams, S.L., Yoon, G., Chitayat, D., Lansdorp, P., Dokal, I., and Dror, Y. (2008). Ataxia and pancytopenia caused by a mutation in TINF2. Hum. Genet. *124*, 507–513.

van Steensel, B., and de Lange, T. (1997). Control of telomere length by the human telomeric protein TRF1. Nature *385*, 740–743.

Verdun, R.E., Crabbe, L., Haggblom, C., and Karlseder, J. (2005). Functional human telomeres are recognized as DNA damage in G2 of the cell cycle. Mol. Cell *20*, 551–561.

Walne, A.J., Vulliamy, T., Beswick, R., Kirwan, M., and Dokal, I. (2008). TINF2 mutations result in very short telomeres: analysis of a large cohort of patients with dyskeratosis congenita and related bone marrow failure syndromes. Blood *112*, 3594–3600.

Wang, F., Podell, E.R., Zaug, A.J., Yang, Y., Baciu, P., Cech, T.R., and Lei, M. (2007). The POT1-TPP1 telomere complex is a telomerase processivity factor. Nature *445*, 506–510.

Wold, M.S. (1997). Replication protein A: a heterotrimeric, single-stranded DNA-binding protein required for eukaryotic DNA metabolism. Annu. Rev. Biochem. *66*, 61–92.

Wold, M.S., and Kelly, T. (1988). Purification and characterization of replication protein A, a cellular protein required for in vitro replication of simian virus 40 DNA. Proc. Natl. Acad. Sci. USA *85*, 2523–2527.

Wu, L., Multani, A.S., He, H., Cosme-Blanco, W., Deng, Y., Deng, J.M., Bachilo, O., Pathak, S., Tahara, H., Bailey, S.M., et al. (2006). Pot1 deficiency initiates DNA damage checkpoint activation and aberrant homologous recombination at telomeres. Cell *126*, 49–62.

Xin, H., Liu, D., Wan, M., Safari, A., Kim, H., Sun, W., O'Connor, M.S., and Songyang, Z. (2007). TPP1 is a homologue of ciliate TEBP-beta and interacts with POT1 to recruit telomerase. Nature *445*, 559–562.

Xu, X., Vaithiyalingam, S., Glick, G.G., Mordes, D.A., Chazin, W.J., and Cortez, D. (2008). The basic cleft of RPA70N binds multiple checkpoint proteins, including RAD9, to regulate ATR signaling. Mol. Cell. Biol. *28*, 7345–7353.

Yang, Q., Zheng, Y.L., and Harris, C.C. (2005). POT1 and TRF2 cooperate to maintain telomeric integrity. Mol. Cell. Biol. *25*, 1070–1080.

Ye, J.Z., and de Lange, T. (2004). TIN2 is a tankyrase 1 PARP modulator in the TRF1 telomere length control complex. Nat. Genet. *36*, 618–623.

Ye, J.Z., Donigian, J.R., van Overbeek, M., Loayza, D., Luo, Y., Krutchinsky, A.N., Chait, B.T., and de Lange, T. (2004a). TIN2 binds TRF1 and TRF2 simultaneously and stabilizes the TRF2 complex on telomeres. J. Biol. Chem. *279*, 47264–47271.

Ye, J.Z., Hockemeyer, D., Krutchinsky, A.N., Loayza, D., Hooper, S.M., Chait, B.T., and de Lange, T. (2004b). POT1-interacting protein PIP1: a telomere length regulator that recruits POT1 to the TIN2/TRF1 complex. Genes Dev. *18*, 1649–1654.

Zhao, Y., Hoshiyama, H., Shay, J.W., and Wright, W.E. (2008). Quantitative telomeric overhang determination using a double-strand specific nuclease. Nucleic Acids Res. *36*, e14.

Zou, L., and Elledge, S.J. (2003). Sensing DNA damage through ATRIP recognition of RPA-ssDNA complexes. Science *300*, 1542–1548.